ORIGINAL RESEARCH

Suppressive effects of electrochemically reduced water on matrix metalloproteinase-2 activities and in vitro invasion of human fibrosarcoma HT1080 cells

Tomoya Kinjo · Jun Ye · Hanxu Yan · Takeki Hamasaki · Hidekazu Nakanishi · Kazuko Toh · Noboru Nakamichi · Shigeru Kabayama · Kiichiro Teruya · Sanetaka Shirahata

Abstract It has been demonstrated that hydrogen peroxide (H_2O_2) is directly associated with elevated matrix metalloproteinase-2 (MMP-2) expression in several cell lines. Electrochemically reduced water (ERW), produced near the cathode during electrolysis, and scavenges intracellular H_2O_2 in human fibrosarcoma HT1080 cells. RT-PCR and zymography analyses revealed that when HT1080 cells were treated with ERW, the gene expression of MMP-2 and membrane type 1 MMP and activation of MMP-2 was repressed, resulting in decreased invasion of the cells into matrigel. ERW also inhibited H_2O_2-induced MMP-2 upregulation. To investigate signal transduction involved in MMP-2 downregulation, mitogen-activated protein kinase (MAPK)-specific inhibitors, SB203580 (p38 MAPK inhibitor), PD98059 (MAPK/extracellular regulated kinase kinase 1 inhibitor) and c-Jun NH_2-terminal kinase inhibitor II, were used to block the MAPK signal cascade. MMP-2 gene expression was only inhibited by SB203580 treatment, suggesting a pivotal role of p38 MAPK in regulation of MMP-2 gene expression. Western blot analysis showed that ERW downregulated the phosphorylation of p38 both in H_2O_2-treated and untreated HT1080 cells. These results indicate that the inhibitory effect of ERW on tumor invasion is due to, at least in part, its antioxidative effect.

T. Kinjo · H. Yan · H. Nakanishi · K. Teruya ·
S. Shirahata
Division of Life Engineering, Graduate School of Systems
Life Sciences, Kyushu University, 6-10-1 Hakozaki,
Higashi-ku, Fukuoka 812-8581, Japan

J. Ye · T. Hamasaki · K. Toh · N. Nakamichi ·
K. Teruya · S. Shirahata (✉)
Department of Bioscience and Biotechnology, Faculty
of Agriculture, Kyushu University, 6-10-1 Hakozaki,
Higashi-ku, Fukuoka 812-8581, Japan
e-mail: sirahata@grt.kyushu-u.ac.jp

J. Ye
State Key Laboratory of Cellular Stress Biology, School
of Life Science, Xiamen Universitry, Xiamen, China

S. Kabayama
Nihon Trim Co. Ltd., 1-8-34 Oyodonaka, Kita-ku,
Osaka 531-0076, Japan

Abbreviations

ABTS	2,2-azino-bis-(2-ethylbenzothioazoline-6-sulfonic acid) diammonium salt
AERW	Autoclaved ERW
AsA	Ascorbic acid
Bes-H_2O_2	3′-O-acetyl-6′-O-pentafluorobenzene sulfonyl-2′,7′-difluorofluorescein
ERW	Electrochemically reduced water
FBS	Fetal bovine serum
JNK	c-Jun NH_2-terminal kinase
JNKi	JNK inhibitor II

MAPK	Mitogen-activated protein kinase
MEM	Modified Eagle's medium
MMP	Matrix metalloproteinase
MT1-MMP	Membrane type 1-MMP
NAC	N-acetyl cysteine
PMS	Phenazine methosulfate
POD	Streptavidin-horseradish peroxidase conjugate
ROS	Reactive oxygen species
SDS	Sodium dodecyl sulfate
TIMP2	Tissue inhibitor of metalloproteinase 2

Introduction

The ability to invade tissues and establish secondary tumors in remote sites, or "metastasis", is a characteristic of malignant tumor cells and the main cause of most cancer-related deaths in humans. During metastasis, tumor cells must degrade the extracellular matrix and basement membrane to facilitate invasion. Matrix metalloproteinases (MMPs) play a critical role in this process (Kessenbrock et al. 2010). In particular, MMP-2 and MMP-9 are thought to be key enzymes for the degradation of type IV collagen, a major component of the basement membrane (Mook et al. 2004). However, MMP-2 and -9 are secreted from cells as zymogens, and post-translational modifications are required for MMP-2 and -9 activation and acquisition of proteolytic function upon interaction with membrane type 1-MMP (MT1-MMP) and tissue inhibitor of metalloproteinase 2 (TIMP2) (Sternlicht and Werb 2001). Numerous studies have documented a direct correlation between high levels of hydrogen peroxide (H_2O_2) and enhanced MMP-2 expression and activation, which is a characteristic of most malignant tumors (Yoon et al. 2002; Zhang et al. 2002; Kim et al. 2007; Kessenbrock et al. 2010). Many cancer cells have been shown to produce large amounts of reactive oxygen species (ROS) including hydrogen peroxide (H_2O_2) (Szatrowski and Nathan 1991). ROS are involved in metastatic processes including invasion of cancer cells into the surrounding primary tumor site by remodeling the extracellular matrix with MMPs and other factors (Wu 2006). Pathway schematics, in which generated ROS regulates tumor progression, indicate that ROS is situated upstream in many signaling pathways including the pathway involved in up-regulation of MMPs for cell invasion (Nelson

and Melendez 2004; Wu 2006; Liou and Storz 2010). At the tumor site, a large amount of ROS, produced by activated neutrophils and macrophages in the inflammatory response, has been shown to activate MMPs by oxidation of the pro-domain cysteine (Kessenbrock et al. 2010). Sustained H_2O_2 production has been shown to activate MMP-2 in HT-1080 cells (Yoon et al. 2002). Sublethal H_2O_2 exposure to human endothelial cells increases the expression of MMP-2 (Belkhiri et al. 1997). Furthermore, changes in ROS production have been evaluated for modulation of MMP-2 activation, and it was found that ciglitazone-activated pro-MMP-2 is caused by sustained production of ROS (Kim et al. 2007). MMP-2 activation by overexpression of manganese superoxide dismutase in human breast cancer MCF-7 is mediated by H_2O_2 (Zhang et al. 2002). Recently, oxidative stress due to ROS, including H_2O_2, and cancer progression were reported to be elicited by MT1-MMP (Nguyen et al. 2011). Culture medium with a negative redox potential (e.g., –180 mV) suppresses tumor invasion, revealing that the extra- and intra-cellular redox balance regulates the invasion of cancer cells (Ortega et al. 2010; Chaiswing et al. 2012).

Electrochemically reduced water (ERW) produced near the cathode during water electrolysis exhibits high pH, low dissolved oxygen and an extremely negative redox potential (e.g., −800 mV) (Shirahata et al. 1997). ERW contains a high concentration of dissolved hydrogen and a small amount of Pt nanoparticles, both of which exhibit ROS-scavenging effects (Ye et al. 2008; Hamasaki et al. 2008; Li et al. 2011; Shirahata et al. 2012). It has been demonstrated that neutralized ERW has a H_2O_2-scavenging ability, which is thought to be associated with several protective functions against oxidative damage such as DNA and mitochondrial damage (Shirahata et al. 1997; Tsai et al. 2009a, b), lifespan extension of *Caenorhabditis elegans* (Yan et al. 2010; 2011), alloxan-induced type 1 diabetes (Li et al. 2002, 2011), and hemodialysis-induced oxidative stress during end-stage renal disease (Huang et al. 2003). ERW exhibits a variety of physiological functions by several mechanisms via its antioxidative properties (Shirahata et al. 2012).

The highly metastatic human fibrosarcoma HT1080 cell line, which secretes several MMPs, is one of the most popular cell lines to study invasiveness (Fisher et al. 2006). Previously, we reported that ERW can scavenge ROS, such as H_2O_2, in the hamster

pancreatic β-cell line HIT-T15 (Li et al. 2002, 2011) and rat L6 myotube cells (Oda et al. 1999). ERW has been shown to induce differentiation of K562 human leukemia cells into megakaryocyte (Komatsu et al. 2004). We also reported that ERW can inhibit tumor angiogenesis using human lung carcinoma A549 cells (Ye et al. 2008). ERW supplemented with Pt nanoparticles has been also shown to inhibit two-stage cell transformation of Balb/c 3T3 A31-1-1 cells (Nishikawa et al. 2005). Furthermore, we reported that ERW contributes to extension of the *Caenorhabditis elegans* lifespan, and ERW improves the symptoms of diabetes mellitus in ICR (CD-1 strain) mice (Yan et al. 2010; Yan et al. 2011; Li et al. 2011). Here, we demonstrate that ERW inhibits both MMP-2 and MT1-MMP gene expression and activation of MMP-2 in HT1080 cells, thereby suppressing in vitro cell invasion.

Materials and methods

Preparation of ERW and reagents

ERW was prepared by electrolysis of ultrapure water containing 2 mM NaOH at 100 V for 60 min using an electrolyzing device equipped with Pt-coated Ti electrodes (TI-200 s; Nihon Trim Co, Osaka, Japan). The electrolyzing device was a batch type one and consisted of a 4 L vessel (190 mm long × 210 mm wide × 140 mm high) divided by a semi-permeable membrane (190 mm wide × 130 mm high). Two rectangular Pt-coated Ti electrode plates (70 mm × 110 mm) were set at a distance of 27.5 mm from the membrane. Matrigel was purchased from Funakoshi (Tokyo, Japan). Streptavidin-horseradish peroxidase conjugate (POD) was purchased from GE Health Care (Tokyo, Japan). SB203580, PD98059 and c-Jun NH$_2$-terminal kinase (JNK) inhibitor II (JNKi) were obtained from Calbiochem (San Diego, CA). 3′-O-acetyl-6′-O-pentafluorobenzenesulfonyl-2′,7′-difluorofluorescein (BES-H$_2$O$_2$), 2,2-azino-bis-(2-ethyl-benzothioazoline-6-sulfonic acid) diammonium salt (ABTS), phenazine methosulfate (PMS), ascorbic acid (AsA), and N-acetyl cysteine (NAC) were purchased from Wako (Osaka, Japan). Anti-total and phospho-p38 mitogen-activated protein kinase (MAPK) antibodies were obtained from Cell Signaling Technology Japan (Tokyo, Japan). Ultrapure water (MQ) was prepared using a Milli-Q integral system (Millipore, Billerica, MA).

Preparation of ERW-containing medium and cell culture

A closed capped glass bottle was filled with freshly prepared ERW and stored in an inverted position to avoid loss of dissolved hydrogen before preparation of ERW-containing medium. Five times concentrated modified Eagle's medium (MEM) prepared using ultrapure water was diluted 5-fold with freshly prepared ERW or ultrapure water for ERW-containing medium and control medium, respectively. Medium was immediately sterilized by filtration through a 0.2 μm filter under applied pressure. ERW-containing medium was stored in a closed capped glass bottle at 4 °C before use. To inactivate active substances in ERW, ERW was autoclaved in an open glass bottle at 120 °C for 20 min to prepare autoclaved ERW (AERW)-containing medium. HT1080 cells (CCL-121; American Type Culture Collection, Manassas, VA, USA), a human fibrosarcoma cell line, were cultured in control or ERW-containing medium supplemented with 10 % fetal bovine serum (FBS; Funakoshi, Tokyo, Japan). Alkaline ERW was neutralized by the addition of HEPES buffer to the medium before use. H$_2$O$_2$, PMS, SB203580, PD98059 and JNKi were added to culture medium directly.

Assessment of the amount of intracellular H$_2$O$_2$

HT1080 cells were seeded into a 96 well plate at 1×10^5 cells/well. After 12 h of culture in MEM supplemented with 10 % FBS, medium was changed to control- or ERW-medium without FBS, and cells were cultured with or without H$_2$O$_2$ for 24 h. Cells were then incubated with 5 μM BES-H$_2$O$_2$ and 1 μM Hoechst 33342 for 15 min. The relative fluorescence intensity of BES-H$_2$O$_2$ indicating intracellular H$_2$O$_2$ in each cell was determined by an In Cell Analyzer 1000 (GE Healthcare, Tokyo, Japan) with an excitation filter at 480 nm and an emission filter at 535 nm. Data derived from 1,350 cells were statistically analyzed. The In Cell Analyzer 1000 could rapidly and quantitatively determine the fluorescence intensity of BES-H$_2$O$_2$ in each cell to provide statistically reliable data derived from several thousands to several million cells.

Gelatin zymography

HT1080 cells were cultured in MEM supplemented with 10 % FBS overnight and then treated with ERW, AERW or 5 mM NAC-containing serum-free MEM with or without 2 μM PMS for 24 h. Conditioned medium was then collected and concentrated with centrifugal filter devices (Millipore, MA). Ten micro-liter aliquots of conditioned medium were mixed with 10 μl sample buffer (0.25 M Tris–HCl, pH 6.0, 8.5 % glycerol, 4 % sodium dodecyl sulfate (SDS) and 0.01 % bromophenol blue). Samples were then elec-trophoresed in a 7.5 % SDS–polyacrylamide gel containing 2 mg/ml gelatin. After electrophoresis, the gel was washed three times for 10 min in 2.5 % Triton X-100 and then placed in incubation buffer (50 mM Tris–HCl, pH 7.6, 10 mM $CaCl_2$, 50 mM NaCl and 0.05 % Brij 35) overnight at 37 °C. After incubation, the gel was stained with a solution of 0.25 % Coomassie blue R250, 40 % methanol and 10 % acetic acid for 1 h at room temperature and then destained with 40 % methanol and 10 % acetic acid until protein bands were apparent.

Matrigel invasion assay

A Falcon 24 well plate was coated with 700 μl serum-free MEM containing 10 μg fibronectin (Sigma-Aldrich, St Louis, MO). Eight micrometer chambers (Kurabo, Osaka, Japan) were coated with 20 μl 1:6 diluted matrigel (2.5 mg protein/ml) for 30 min and then inserted into the 24 well plate. HT1080 cells were pre-cultured in medium containing ERW, AERW or 5 mM NAC for 24 h, seeded at 1×10^5 cells/well into the chambers and then incubated for 16 h at 37 °C. In the lower chamber, MEM containing 10 % FBS served as the source of chemoattractants. Cells that invaded into the lower surface of the matrigel were fixed with 99 % methanol and stained with Diff-Quik (Sysmex, Kobe, Japan). Invaded cells in three ran-domly selected fields were counted under a light microscope. The invasion ratio was calculated as the percentage of the average number of invaded cells divided by the average number of cells that moved through the control insert membrane. For H_2O_2-treated HT1080 cells, cells were seeded at 1×10^5 cells/well on matrigel in the inner chamber and then incubated in serum-free MEM containing ERW and 0, 10 or 20 μM H_2O_2 for 24 h before determining the invasion ratio. A NaOH solution with the same pH as ERW was used as a control solution and was neutralized with HEPES.

Determination of H_2O_2 in ERW and/or medium

The concentration of H_2O_2 in ERW was determined using a previously reported method (Shirahata et al. 1997). Briefly, a POD-ATBS solution was prepared by mixing 0.2 M citrate buffer (pH 4.0), MQ, an ABTS solution (6 mg/ml) and a POD solution at the ratio of 150:84.7:15:0.3. Fifty microliters of sample water was placed in a well of a 96-well microplate (Nunc), and then 250 μl POS-ABTS solution was added. After mixing for 5 min at 37 °C with a vortex mixer, the absorbance at 405 nm (reference 492 nm) was deter-mined by a microplate reader (Tecanspectra, Wetzlar, Germany).

RT-PCR

Total RNA was isolated using a GenElute^{TM} Mam-malian Total RNA kit (Sigma-Aldrich) following the manufacturer's instructions. Primer sequences for RT-PCR were glyceraldehyde 3-phosphate dehydroge-nase (GAPDH): 5′ACCACAGTCCATGCCATCA C3′ (forward), 5′TCCACCACCCTGTTGCTGTA3′ (reverse); MMP-2: 5′TTCTATGGCTGCCCCAAGG AGAGCTGCAAC3′ (forward), 5′CAGCTCAGCAG CCTAGCCAGTCGGATTTGA3′ (reverse); MT1-MMP: 5′AGGTGATCATCATTGAGGTGG3′ (for-ward), 5′ACAGAGAGAAGCAAGGAGGC3′ (reverse); and TIMP2: 5′AGGGCCAAAGCGGTCAGT3′ (for-ward), 5′CCTGCTTATGGGTCCTCGA-3′ (reverse). PCR conditions were initial denaturation at 94 °C for 3 min, followed by 30 cycles of 94 °C for 30 s, 58 °C for 30 s and 72 °C for 1 min for GAPDH; 30 cycles of 94 °C for 45 s, 60 °C for 45 s and 72 °C for 1 min for MMP-2 and MT1-MMP; and 30 cycles of 94 °C for 45 s, 58 °C for 45 s and 72 °C for 1 min for TIMP2.

Western blot analysis

Cells were washed with phosphate-buffered saline (PBS; pH 7.4), incubated with extraction buffer (50 mM Tris, pH 7.5, 150 mM NaCl, 1 mM phenyl-methylsulfonyl fluoride, 1 % NP-40, 0.1 % sodium dodecyl sulfate (SDS), 10 μg/ml aprotinin and 10 mM ethylene diamine tetra acetic acid) on ice and then

collected with a scraper. Lysates were centrifuged at 12,000 g for 5 min. Protein samples (30 μg) were diluted at 3:1 with sample buffer (250 mM Tris–HCl, pH 6.8, 40 % glycerol, 20 % beta-mercaptoethanol, 8 % SDS and 0.04 % bromophenol blue), boiled and then electrophoresed in a 10 % SDS–polyacrylamide gel. Proteins were then transferred onto Hybond-ECL membranes (Amersham Pharmacia Biotech, Tokyo, Japan) that were then blocked with 5 % Tween 20-PBS (TBS) containing 10 % skim milk powder (Wako, Osaka, Japan) and probed with primary antibodies followed by peroxidase-coupled secondary antibodies. After washing three times with TBS, membranes were developed using an ECL plus Western Blotting Detection System (Amersham Biosciences, Tokyo, Japan).

Statistics

Three to four independent repeats were conducted for all experiments. Data were presented as the mean ± standard deviation (SD). Statistical significance was determined by the Student's t test and a p value of < 0.05 was considered significant.

Results and discussion

ERW decreases intracellular H_2O_2 in HT1080 cells

To examine the effect of ERW on highly metastatic HT1080 cells, the amount of intracellular H_2O_2 was determined using BES-H_2O_2, a fluorescent probe that more specifically detects intracellular H_2O_2 than 2′,7′-dichlorodihydrofluorescein diacetate (Maeda et al. 2004). HT1080 cells were cultured in control or ERW-containing medium in the presence of 0, 20 or 40 μM H_2O_2 for 24 h, and then the amount of intracellular H_2O_2 was determined by an In Cell Analyzer. As shown in Fig. 1a, the relative amount of increased intracellular H_2O_2 was dependent on the concentration of H_2O_2, suggesting that extracellular H_2O_2 penetrated into cells through the cell membrane and directly increased intracellular H_2O_2 or indirectly stimulated the production of intracellular H_2O_2. Whereas, H_2O_2-treated HT1080 cells cultured in ERW-containing medium exhibited significantly lower intracellular H_2O_2 levels than cells in control medium, indicating that ERW scavenged intracellular H_2O_2 in H_2O_2-

treated HT1080 cells ($p < 0.05$, $p < 0.01$). The scavenging effect of ERW on intracellular ROS has also been reported in other cell lines such as pancreatic β HIT-T15 cells (Li et al. 2002) and human adenocarcinoma A549 cells (Ye et al. 2008).

ERW contains two active substances as ROS scavengers; hydrogen molecules and Pt nanoparticles. Hydrogen molecules are known to scavenge ROS and enhance the gene expression of antioxidant enzymes such as SOD, catalase and HO-1 (Shirahata et al. 2011). Furthermore, Tsai et al. (2009a, b) reported that ERW restores the activities of SOD, catalase, and glutathione peroxidase, which were reduced by CCl_4-induced liver damage in mice. They proposed that ERW acts as an antioxidant and a ROS scavenger. In this study, we determined the concentration of dissolved hydrogen molecules after preparation to examine whether ERW contained enough hydrogen molecules. As shown in Fig. 2c, freshly prepared ERW contained 0.76 ppm hydrogen molecules that gradually decreased to 0.22 ppm after 3 h. Based on the data, the estimated half-life of dissolved hydrogen molecules is approximately 100 min. Fujita et al. (2009) reported that 0.08 ppm dissolved hydrogen molecules is enough to exhibit anti-neurodegenerative effects in a model of neurodegenerative disease in mice. This observation suggests that hydrogen molecules in MEM containing ERW will exert physiological effects on cultured cells because the cell culture was started within 30 min after preparation of ERW. About 0.15 ppm dissolved hydrogen molecules scavenges intracellular H_2O_2 in rat myotube L6 cells, inducing the gene expression of catalase, glutathione peroxidase and heme oxygenase-1 (Shirahata et al. 2011).

ERW contains Pt nanoparticles derived from Pt-coated Ti electrodes. The amount of Pt nanoparticles determined using ICP-Ms varied from 0.1 to 2.5 ppb in several ERW preparations (Yan et al. 2010; 2011; Li et al. 2011; Shirahata et al. 2012). The amount of Pt nanoparticles is rather variable mainly because Pt-coated Ti-electrodes gradually erode with repeated electrolysis, which liberates less Pt nanoparticles resulting in a reduced ROS scavenging ability (unpublished observation). Pt nanoparticles are multifunctional ROS scavengers that can directly scavenge O_2^-, H_2O_2 and ·OH radicals (Hamasaki et al. 2008; Shirahata et al. 2012). Previously, we used a dry ash method to show uptake of Pt nanoparticles into HeLa cells and

Fig. 1 Effects of ERW on intracellular ROS and the invasive
activity of HT1080 cells. **a** Scavenging effects of ERW on
intracellular H_2O_2. HT1080 cells were cultured in a 96 well plate
in control (*black bar*) medium or ERW-containing (*white bar*)
medium in the presence of 0, 20 or 40 μM H_2O_2 for 24 h. Cells
were then incubated in medium containing BES-H_2O_2 for
15 min. The amount of intracellular H_2O_2 was measured by an
In Cell Analyzer. Data are the mean ± SD of three independent
experiments. * $p < 0.05$, ** $p < 0.01$; Student's *t* test. **b** ERW
inhibits the invasion of HT1080 cells. HT1080 cells pretreated
for 24 h in medium prepared with MQ (control), ERW, AERW
or 5 mM NAC were seeded on matrigel and incubated for a
further 16 h at 37 °C. After removing non-invading cells from
the top of the transwell using a cotton swab, cells that invaded
the matrigel were fixed with 99 % ethanol and stained with Diff-
Quick. Cells in three random fields were then counted under a
light microscope. Data are the mean ± SD of three independent
experiments. * $p < 0.05$; Student's t test. **c** ERW inhibits the
invasion of H_2O_2-stimulated HT1080 cells. HT1080 cells
pretreated with medium prepared as described in **b** and
additionally containing H_2O_2 (0, 10 or 20 μM) were seeded
on matrigel and incubated for 24 h at 37 °C. Subsequent
treatments were the same as described in **b**. Black bar: control
medium, white bar: ERW-containing medium. Data are the
mean ± SD of three independent experiments. * $p < 0.05$; **
$p < 0.01$; Student's *t* test

demonstrated that Pt nanoparticles were taken into
cells in time- and dose-dependent manners (Hamasaki
et al. 2008). A localization study using bright-field
scanning transmission electron microscopy has visu-
alized intracellular Pt nanoparticles (Gehrke et al.
2011). Moreover, scanning electron microscopy in
combination with the focused ion beam milling
method revealed that Pt nanoparticles are taken up
by cells (Pelka et al. 2009). Our data and others
indicate that Pt nanoparticles are taken up by cells.
There are studies addressing cellular uptake mecha-
nisms for nanoparticles, and several mechanisms have
been proposed to explain the uptake of gold and Pt
nanoparticles. These nanoparticles are taken into cells
by phagocytosis (Pelka et al. 2009; Krpetic et al.
2010), endocytosis including receptor-mediated endo-
cytosis (Chithrani 2010; Shan et al. 2011; Zhang et al.
2011; Ma et al. 2011), pinocytosis (Shukla et al. 2005)
or simple diffusion (Taylor et al. 2010). The term
endocytosis includes phagocytosis and pinocytosis
depending on the size of materials taken up by cells.
Phagocytosis occurs for particles larger than 100 nm,
and pinocytosis occurs for particles smaller than
100 nm (Shukla et al. 2005). The sizes of Pt nanopar-
ticles contained in ERW are estimated to be 1–10 nm
(Shirahata et al. 2012), far smaller than 100 nm. Thus,
Pt nanoparticles contained in ERW are likely to be
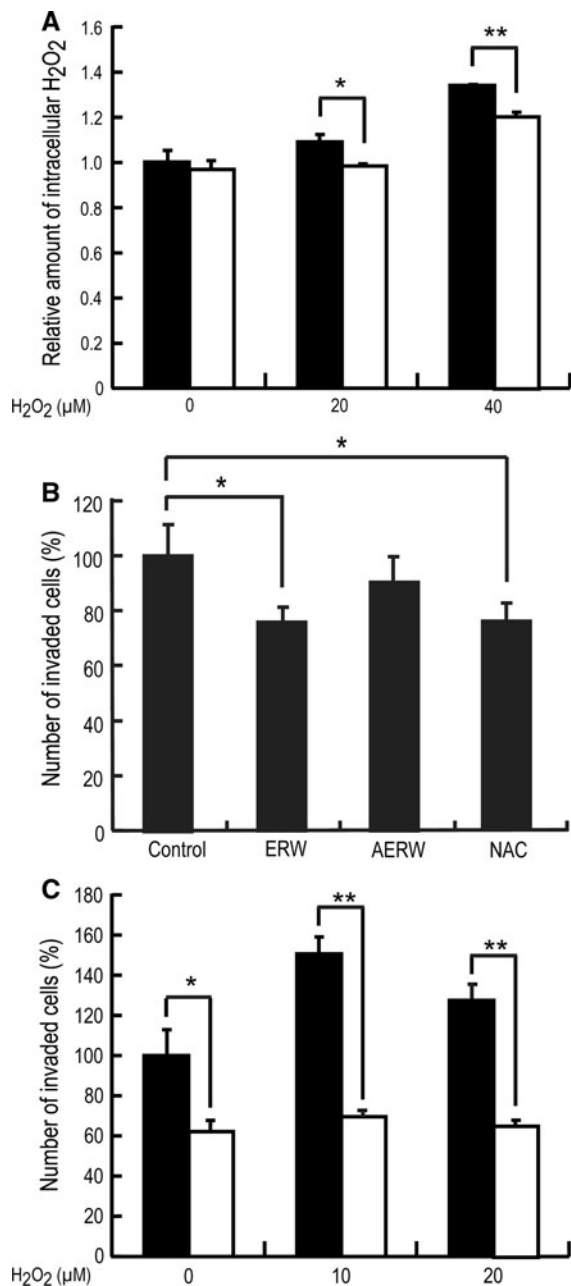
taken up by cells via the pinocytotic process or
combinations of the mechanisms described above.
Once Pt nanoparticles are internalized, particles co-
exist as agglomerated and single primary particle
forms (Gehrke et al. 2011). Interestingly, translocation
of Pt nanoparticles into the nucleus and mitochondria
has not been observed (Shukla et al. 2005; Gehrke
et al. 2011), suggesting that Pt nanoparticles exert
catalase/SOD mimetic and ROS scavenging activities

the dissolved hydrogen concentration in ERW. **a** Time-dependent reduction of H_2O_2 in MQ and ERW. The pH of MQ was adjusted to that of freshly prepared ERW using NaOH (MQ/NaOH). Then, HEPES buffer was added to MQ/NaOH and freshly prepared ERW to adjust pH 7.6. Stock ascorbic acid (AsA; 100 mM) was dissolved in MQ to obtain a final concentration of 100 μM, and the pH was adjusted to 7.6 with HEPES buffer. H_2O_2 (10, 20, 40 and 80 μM) was then added to these solutions. The POD-ATBS method was employed to measure the H_2O_2 concentration with a microplate reader at 0, 0.25, 0.5, 1, 2, 4 and 24 h. Graph designations are as follows: MQ (10): red line with circle, MQ + ASA(10): red line with triangle, ERW(10): red line with square; MQ (20): green line with circle, MQ + ASA(20): green line with triangle, ERW(20): green line with square; MQ (40): blue line with circle, MQ + ASA(40): blue line with triangle, ERW(40): blue line with square; MQ (80): black line with circle, MQ + ASA(80): black line with triangle, ERW(80): black line with square. **b** Time-dependent reduction of H_2O_2 by MEM. The POD-ATBS method was employed as described above. MEM (5×) was diluted with MQ to prepare 1 × MEM/MQ. A stock ASA solution (100 mM) was added to 1 × MEM to obtain a final concentration of 100 μM (MQ/MEM/ASA). MEM (5×) was diluted with ERW to obtain 1 × MEM/ERW. Graph designations are as follows: MQ/MEM (10): red line with circle, MQ/MEM/ASA (10): red line with triangle, ERW/MEM (10): red line with square; MQ/MEM (20): green line with circle, MQ/MEM/ASA (20): green line with triangle, ERW/MEM (20): green line with square; MQ/MEM (40): blue line with circle, MQ/MEM/ASA (40): blue line with triangle, ERW/MEM(40): blue line with square; MQ/MEM (80): black line with circle, MQ/MEM/ASA (80): black line with triangle, ERW/MEM (80): black line with square. The number in parenthesis means the concentration of H_2O_2 (μM). **c** Measurement of hydrogen concentration in ERW. ERW was prepared as described in "Materials and methods". Immediately after electrolysis, ERW was gently collected in a beaker and the dissolved hydrogen concentration was immediately measured using a detector (DM10 type; Biot Co. Ltd, Tokyo, Japan). Then, samples were collected as described above every 30 min up to 180 min. The results of three independent experiments were analyzed by the Student's t test (values are the mean ± SD, n = 3). (Color figure online)

in the cytosolic compartment. However, possible movement of Pt nanoparticles into the nucleus and mitochondria was not excluded due to the detection limit (Gehrke et al. 2011).

Next, we attempted to estimate the number of Pt nanoparticles taken up by a single cell. Previously, we calculated the molecular weight (MW) of 1 and 3 nm Pt nanoparticles based on the assumption that the MW of nanoparticles could be calculated using molar concentration (Hamasaki et al. 2008). The calculated MW of Pt nanoparticles is 10,730 and 276,052 for 1 and 3 nm particles, respectively. We estimated the MW of 2 nm Pt nanoparticles as 143,391 by
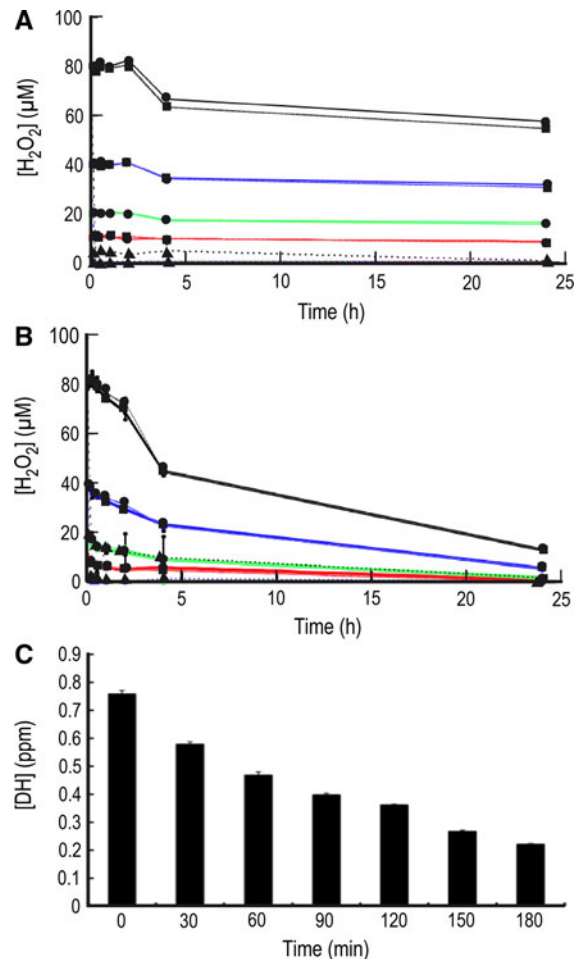
calculating the average MW value between 1 nm and 3 nm Pt nanoparticles. In addition, the intracellular amount of Pt nanoparticles was estimated to be 2×10^{-15} g/cell (Hamasaki et al. 2008). Incorporating these MWs, Avogadro's number and the amount of intracellular Pt nanoparticles, the calculated numbers of Pt nanoparticles per cell are 112×10^3, 8.37×10^3 and 4.35×10^3 particles for 1, 2 and 3 nm Pt nanoparticles, respectively. In addition, we attempted to calculate intracellular particle numbers using published data (Yoshihisa et al. 2011). Again, using basic numbers as described above and replacing the intracellular amount of Pt nanoparticles with 5.6×10^{-16} g/cell (Yoshihisa et al. 2011), the calculated numbers of Pt nanoparticles per cell are 31.3×10^3, 2.34×10^3 and 1.22×10^3 particles for 1, 2 and 3 nm Pt nanoparticles, respectively. These numbers are relatively comparable between the two independent

reports and thus suggest that, although a very rough estimate, Pt nanoparticles are taken up at 100–10,000 particles per cell. However, it should be noted that experiments with synthetic Pt nanoparticles usually apply ppm orders of nanoparticles, whereas ERW contains a ppb order of nanoparticles (Yan et al. 2010; Shirahata et al. 2012). Therefore, the number of Pt nanoparticles in ERW which is taken up by a single cell is estimated to be much smaller. Although the calculated intracellular number of Pt nanoparticles appears to be small, Pt nanoparticles in the cells of nematodes exert a ROS scavenging action (Yan et al. 2011), and activate antioxidative enzymes (Tsai et al. 2009a, b). Two mechanisms can be considered for ERW directly scavenging intracellular ROS or indirectly scavenging intracellular ROS by induction of ROS-scavenging enzymes such as SOD, catalase and peroxidases.

To examine whether ERW can directly scavenge H_2O_2, we determined the concentration of H_2O_2 in ERW. As shown in Fig. 2a, 10, 20, 40 and 80 μM H_2O_2 were rather stable in both MQ and ERW. ERW did not lower the concentration of H_2O_2 even after 24 h. In MEM, the concentration of H_2O_2 gradually decreased and was about one-sixth after 24 h. Again, ERW did not lower the concentration of H_2O_2 in MEM (Fig. 2b).

We used MEM, which contained inorganic components, amino acids, vitamins and other components. The defined ERW used here contains NaOH, NaCl, H_2, and a small amount of minerals like Pt nanoparticles. H_2 is a very weak reductant and will not react with the components of MEM. A small amount of Pt nanoparticles (ppb levels) will not also affect large amounts of the components of the medium.

ERW inhibits the invasion of HT1080 cells

Highly metastatic malignant cells generally exhibit high levels of intracellular ROS (Ladiges et al. 2010; Dayem et al. 2010). Malignant cancer cells secrete MMPs and cause degradation of collagens surrounding cells to facilitate invasion. The invasive activities of cancer cells can be evaluated by a matrigel invasion assay. HT1080 cells were incubated in control and ERW-, AERW- or NAC-containing medium for 24 h and then seeded onto matrigel followed by further culturing for 16 h. As shown in Fig. 1b, when HT1080 cells were treated with ERW, the number of cells invaded into the matrigel was significantly decreased compared with that of control cells ($p < 0.05$). Five

millimolar NAC also suppressed invasion, indicating that the assay system was working properly ($p < 0.05$). Although NAC was used as a system control in this experiment, mechanisms of the anti-invasive activity of NAC may partly share those of ERW. NAC is a precursor of L-cysteine and thus of reduced glutathione, and a ROS scavenger (Aruoma et al. 1989; Albini et al. 1995; Zafarullah et al. 2003). Molecular mechanisms of NAC show that it inhibits multiple signaling pathways in cells (Zafarullah et al. 2003). Anti-oxidant effects of NAC are due to reacting with hydroxyl radicals and H_2O_2 (Aruoma et al. 1989).This antioxidative activity has been reported to be the result of an increased cellular glutathione concentration induced by NAC (Kyaw et al. 2004). Another report suggested that an activity of NAC is inhibition of cancer cell invasion and metastasis by inhibiting MMP-2 and MMP-9 (Albini et al. 1995; Cai et al. 1999; Zafarullah et al. 2003). Because NAC exhibits multifaceted activities in cells, NAC in Fig. 1b was used as a system control. Under the condition in which the system control worked properly, the suppressive effect of ERW on invasion was demonstrated ($p < 0.05$). This result can be explained by two properties of ERW. Accumulated data suggest that ERW functions as an antioxidant and ROS scavenger (Ye et al. 2008; Tsai et al. 2009a, b; Li et al. 2011). To explain its activities, we have proposed a working hypothesis of the active hydrogen theory in which ERW produces active hydrogen (hydrogen atoms) with a high reducing potential, resulting in a ROS scavenging activity (Shirahata et al. 1997, 2012; Shirahata 2002). To advance our understanding of ERW activity, we theorized that Pt nanoparticles, liberated from the Pt-coated Ti electrode during electrolysis, play a pivotal role in the ROS scavenging activity in a NaOH-derived model ERW. We analyzed the components in a 2 mM NaOH solution and ERW using an inductively coupled plasma mass spectrometer (ICP-Ms), and reported that only Pt and Pt components in ERW are increased by approximately 20-fold compared with that of a 2 mM NaOH solution from which ERW was produced (Li et al. 2011, supplementary material Table 3; Shirahata et al. 2012). Furthermore, we synthesized Pt nanoparticles that were found to scavenge ROS (Hamasaki et al. 2008). Considering these results, we proposed a modified hypothesis, that is, an active hydrogen mineral nanoparticle reduced water hypothesis of

reduced water containing metal nanoparticles and hydrogen molecules (Ye et al. 2008; Shirahata et al. 2012). Electrolysis of water containing mineral ions simultaneously produces both metal nanoparticles including Pt nanoparticles and hydrogen molecules on the Pt-coated Ti electrodes. Active hydrogen is continuously generated from hydrogen molecules by the catalytic activity of Pt nanoparticles (Minaev and Ågren 1999; Isobe et al. 2003; Hamasaki et al. 2008). Thus, at least two mechanisms are thought to be involved in ERW activity, whereby Pt nanoparticles alone can show a ROS scavenging activity and active hydrogen adsorbed/absorbed to Pt nanoparticles can act as a ROS scavenger. In support of this hypothesis, results related to ours using synthetic Pt nanoparticles have been reported, which show its ROS scavenging activity (Kajita et al. 2007; Kim et al. 2008; Yoshihisa et al. 2011). On the other hand, AERW exhibited a decreased suppressive effect on invasion (Fig. 1b), indicating that active substances in ERW may be heat-unstable or volatile. These results were consistent with those reported previously (Li et al. 2002). ERW mainly contains Pt nanoparticles and hydrogen molecules, and is likely to contain Pt nanoparticles with adsorbed active hydrogen converted from hydrogen molecules by the catalytic action of Pt nanoparticles (Minaev and Ågren 1999; Roucoux et al. 2002; Isobe et al. 2003; Li et al. 2011; Supplementary material Table 3; Shirahata et al. 2012). We have reported that autoclaving synthetic Pt nanoparticles will agglomerate Pt nanoparticles, as visualized by transmission electron microscopy (Hamasaki et al. 2008). Thus, autoclaving Pt nanoparticles in ERW is assumed to cause agglomeration of Pt nanoparticles under the conditions used (121 °C, 20 min and 860–1,060 hPa), resulting in loss of its activity mainly due to inefficient cellular uptake. In addition, autoclaving ERW might forcefully expel dissolved hydrogen molecules and active hydrogen adsorbed/absorbed in Pt nanoparticles, thereby further reducing its effect, although more evidences have to be accumulated to test this hypothesis.

We performed further experiments to evaluate the effect of ERW on the invasiveness of H_2O_2-treated HT1080 cells as shown in Fig. 1c. In this experiment, H_2O_2 was used to promote invasion in the presence or absence of ERW to evaluate whether invasion could be suppressed. Ten and 20 μM H_2O_2 stimulated the invasion of HT1080 cells, and ERW significantly

suppressed invasion as shown in Fig. 1c ($p < 0.05$ or $p < 0.01$). Concentrations higher than 20 μM H_2O_2 exhibited severe cytotoxicity (data not shown), suggesting that a lower number of invaded cells at 20 μM H_2O_2 might be due to the cytotoxicity of H_2O_2. ERW suppressed the invasion of H_2O_2-treated HT1080 cells more effectively than that of non-treated HT1080 cells. Intracellular ROS levels in H_2O_2-treated HT1080 cells were significantly lower compared with those in non-treated HT1080 cells (Fig. 1a). These results suggest that ERW suppresses intracellular ROS levels and the invasion of oxidative stress-received cancer cells more effectively than those of non-oxidative stress-received cancer cells.

Here we noted Pt nanoparticles only in ERW prepared from a 2 mM NaOH solution using Pt-coated Ti electrodes as a model water of ERW. Based on many researches on safety and efficiency to produce hydrogen molecules, Pt-coated Ti electrodes have been chosen to produce many commercial apparatus. However, ERW prepared from tap water using Pt or different electrodes, which many consumers are daily drinking, will contain a variety of mineral nanoparticles and mineral nanoparticle hydrides produced from various mineral ions in tap water, because electrochemical reduction is one of common methods to produce mineral nanopaticles and nanoparticle hydrides (Watzky and Finke 1997; Aiken and Finke 1999). Physiological functions of nanoparticles and nanoparticle hydrides in ERW derived from tap water remains to be investigated in the future.

ERW inhibits the gene expression of MMP-2 and MT1-MMP and the activation of MMP-2

Thus far, many potential transcription factor binding sites have been found in the MMP-2 promoter, and p53 (Bian and Sun 1997), AP2 and SP1 (Qin et al. 1999) are thought to be particularly essential for MMP-2 expression, although other transcription factors function synergistically to enhance MMP-2 expression (Mook et al. 2004).

MT1-MMP and TIMP2 are critical regulators of MMP-2 activation (Forget et al. 1999). It has been reported that H_2O_2 upregulates MMP-2 gene expression in various cell lines (Yoon et al. 2002).

First, we evaluated the effect of ERW on MMP-2 gene expression in HT1080 cells. As shown in Fig. 3a, ERW attenuated both MMP-2 and MT1-MMP gene

expression in HT1080 cells, but had no significant effect on TIMP2 gene expression. ERW also suppressed MMP-9 gene expression, but MMP-9 gene expression was weak and unstable in HT1080 cells (data not shown). AERW also attenuated MMP-2 gene expression, but the effect was weakened compared with that of ERW (Fig. 3a). We investigated whether H_2O_2 induced upregulation of MMP-2 gene expression in HT1080 cells. As shown in Fig. 3b, MMP-2 gene expression was enhanced in HT1080 cells treated with 10–100 μM H_2O_2. However, 200 μM H_2O_2 treatments resulted in substantially reduced MMP-2 gene expression in HT1080 cells, suggesting that excess oxidative stress suppressed cellular functions. We also investigated whether ERW could inhibit H_2O_2-induced upregulation of MMP-2 gene expression. HT1080 cells were treated with 20 and 40 μM H_2O_2 or both H_2O_2 and ERW for 24 h. Consequently, H_2O_2-induced upregulation of MMP-2 gene expression was inhibited by ERW (Fig. 3c). Pro-MMP-2, intermediate MMP-2 and activated MMP-2 were detected by gelatin zymography as protein bands at 72, 64 and 62 kDa, respectively, (Fig. 3d) as reported by Strongin et al. (1993). PMS, a procyanin analog, is

a strong oxidant that induces intracellular ROS (Shcherbachenko et al. 2007). Direct treatment with extracellular H_2O_2 could not induce pro-MMP-2 activation, whereas intracellular H_2O_2 induced by PMS could induce pro-MMP-2 activation (Yoon et al. 2002). ERW inhibited both extracellular H_2O_2- and PMS-induced MMP-2 activation (Fig. 3c, d).

ERW inhibits MMP-2 gene expression via P38 MAPK inactivation

Antioxidant regulation of MAPK activation and gene expression, which is subject to MAPK, has been reported frequently (Qin et al. 1999; Vayalil et al. 2003; Zafarullah et al. 2003). MAPKs are components of the kinase cascade that connects extracellular stimuli to specific transcription factors, thereby converting these signals into cellular responses. In mammals, there are three MAPKs, namely p38, ERK and JNK, and their activation is correlated with intracellular redox conditions (Adler et al. 1999). Compelling studies have also shown that MMP-2 is a target gene of p38 regulation (Park et al. 2002),
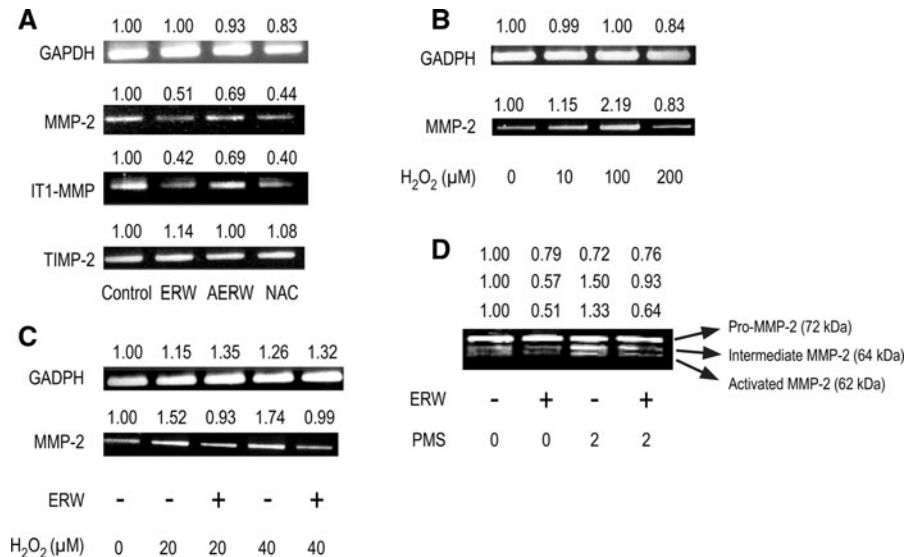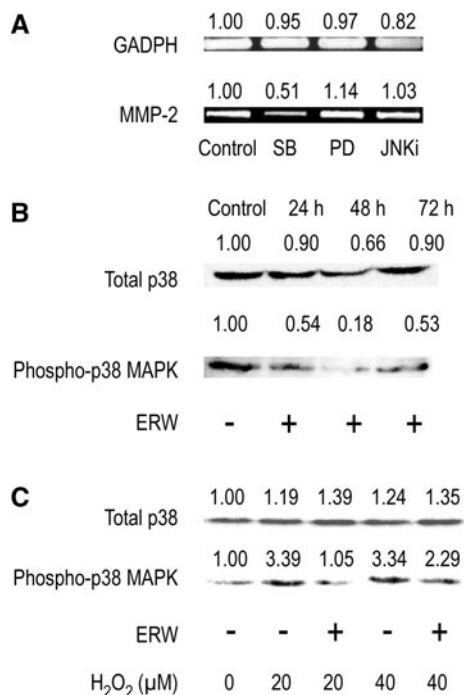

Fig. 3 ERW inhibits MMP-2 and MT1-MMP gene expressions and activation of MMP-1 in HT1080 cells and H_2O_2-treated HT1080 cells. **a** HT1080 cells were treated with serum-free MEM containing ERW, AERW and NAC for 24 h, followed by RT-PCR analysis. **b** HT1080 cells were treated with H_2O_2 for 24 h and RT-PCR was done to detect MMP-2 gene expression. **c** HT1080 cells were treated with H_2O_2 in MEM/MQ or MEM/ERW for 24 h and RT-PCR was done to detect MMP-2

expression. **d** HT1080 cells were cultured in MEM supplemented with 10 % FBS overnight and then treated with MEM containing ERW for 24 h in the presence or absence of 2 μM PMS. Culture supernatants were collected and concentrated, and then zymography was performed. Densitometric analysis was performed using an ImageJ software and the relative values were shown at the upper part of each figures. The results shown are a representative of three independent experiments

indicating the pivotal role of p38 in regulating MMP-2 expression.

To investigate the signal transduction pathway involved in regulating MMP-2 gene expression, MAPK-specific inhibitors, SB203580 (p38 inhibitor), PD98059 (MAPK kinase/ERK inhibitor) and JNKi (JNK inhibitor II), were used. The results showed that only SB203580 blocked MMP-2 gene expression, suggesting a pivotal role of p38 in regulating MMP-2 gene expression in HT1080 cells (Fig. 4a). Further experiments were performed to determine whether ERW-induced downregulation of MMP-2 gene expression was due to inactivation of p38. Western blotting showed that phosphorylation of p38 was also blocked by treatment with ERW (Fig. 4b). Furthermore, ERW also antagonized the enhanced activation of p38 induced by H_2O_2 treatment (Fig. 4c). N-acetyl cysteine, an antioxidant, can inhibit p38 MAPK via redox regulation (Zafarullah et al. 2003). Capsaicin, a cancer-suppressing agent, suppresses the epidermal growth factor-induced invasion of HT1080 cells by inhibiting the expression of MMP-2 and MT1-MMP via inhibition of p38 MAPK (Hwang et al. 2011).

The putative mechanism of the suppressive effect of ERW in HT1080 cells were shown in Fig. 5. ERW suppresses the expression of MMP-2 and MT1-MMP but not of TIMP2 via p38 MAPK inactivation, inhibiting the secretion of ProMMP-2 and activation of MMP-2, which results in suppression of degradation of extracellular matrix and invasion of tumor cells.

Redox deregulation represents a specific vulnerability of malignant cells that can be selectively targeted by redox chemotherapeutics (Wondrak 2009). Many antioxidants are candidates for redox chemotherapeutics. AsA, which is widely used for cancer therapy, generates ROS in cancer cells via redox cycling of exogenous/endogenous copper ions (Hadi et al. 2010). This observation raises a question about the relationship between ROS generation and MMP-2 activation by AsA. Cancer cells are thought to be killed by either elevating or depleting ROS levels (Schumacker 2006; Wang and Yi 2008). AsA is known to act as a pro-oxidant by generating ROS (Duarte et al. 2007; Hadi et al. 2010). In contrast, AsA exhibits anti-proliferative and -invasive effects on hepatoma cells, suggesting an anti-oxidative property of AsA (Hirakawa et al. 2005). In addition, AsA has been used as an agent for anti-oxidant therapy (Wang and Yi 2008). High-dose AsA administered to Balb/c mice implanted with sarcoma 180 cancer cells has been shown to suppress genes involved in angiogenesis (Yeom et al. 2009). In their study, expression of basic fibroblast growth factor, vascular endothelial growth factor and MMP-2 genes was greatly suppressed by AsA. They suggested an alternative anti-tumor mechanism in which tumor growth is inhibited by the angiostatic effects of AsA. Moreover, a nutrient mixture containing AsA, lysine, proline and green tea extract has been demonstrated to inhibit both MMP-2 and MMP-9 expression and activities (Roomi et al. 2011). These studies did not measure ROS levels when MMPs were suppressed. However, based on these studies, reduction of ROS levels and down-regulation of MMPs are likely mechanisms occurring in cells. The anti-cancer effects of ERW have been recently


Fig. 4 ERW suppresses MMP-2 expression via p38 MAPK. **a** HT1080 cells were treated with serum-free MEM containing 10 μM SB (SB203580), 20 μM PD (PD98059) or 40 nM JNKi for 24 h, followed by RT-PCR analysis. HT1080 cells were treated with ERW for 24, 48 and 72 h in the absence of H_2O_2 (**b**) or for 24 h in the presence of H_2O_2 (**c**), followed by western blot analysis. Densitometric analysis was performed using an ImageJ software and the relative values were shown at the upper part of each figures. The results shown are a representative of three independent experiments

Fig. 5 Putative mechanism
of the suppressive effect of
ERW on the invasive
activity of HT1080 cells.
(Color figure online)
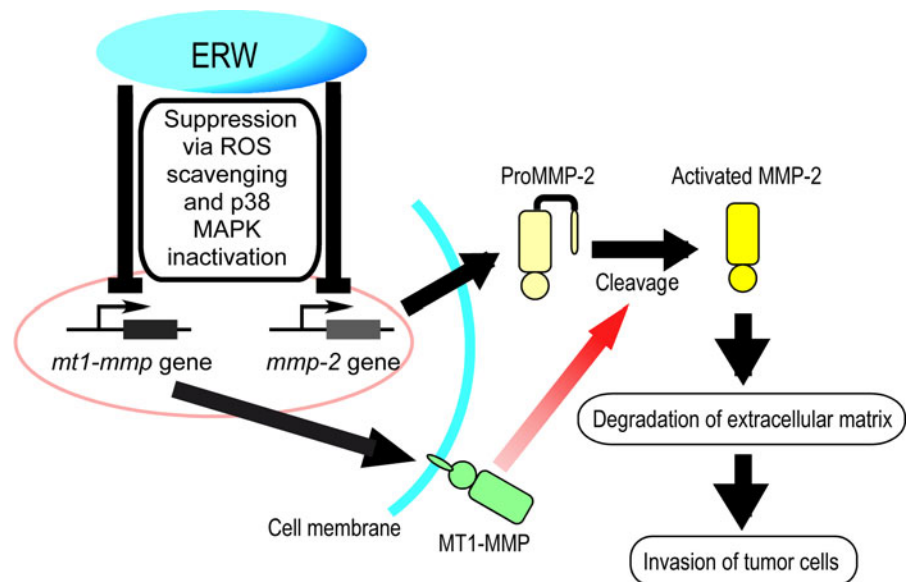
reviewed as described below (Shirahata et al. 2012). ERW causes telomere shortening in cancer cells and suppresses tumor angiogenesis by scavenging intracellular ROS and suppressing the gene expression and secretion of vascular endothelial growth factor. In addition, ERW induces apoptosis together with glutathione in human leukemia HL60 cells (Tsai et al. 2009a, b). ERW also induces differentiation of K562 cells into megakaryocytes (Komatsu et al. 2004). The active agents in ERW responsible for the anticancer effects have not been thoroughly elucidated. Freshly prepared ERW contains a high concentration of dissolved hydrogen at 0.4–0.9 ppm and a ppb level of Pt nanoparticles derived from the Pt-coated Ti electrodes of the electrolyzing device (Yan et al. 2010). Since the inhibiting activity of ERW on invasion was lost by autoclaving, the agents seem to be heat-unstable or volatile. Hydrogen molecules in ERW are one of the candidates. However, despite many reports demonstrating that hydrogen molecules suppress various symptoms of oxidative stress-related disease in animal models (Shirahata et al. 2012), there are few reports on its anti-cancer effects. It is assumed that the antioxidant activity of hydrogen molecules may be too weak to suppress malignant cancer cells. ERW contains a small amount of Pt nanoparticles. Pt nanoparticles are multi-functional ROS scavengers and efficient catalysts for the production of hydrogen atoms, potent reductants, from hydrogen molecules (Shirahata et al. 2012). ERW supplemented with

synthesized Pt nanoparticles strongly suppresses the transformation of NIH3T3 cells by 3-methyl cholanthrene and a phorbol-12-myristate-13 acetate (Nishikawa et al. 2005). Further investigation will be needed to reveal the anticancer effects of Pt nanoparticles and hydrogen atoms.

ERW may impact cellular behaviors of epithelial carcinomas (Roh et al. 2012) and normal (nontransformed) fibroblast (Maxova et al. 2010), both of which are aggressively and actively produce MMP-2. ERW suppressed intracellular ROS level and extracellular H_2O_2 level of cultured human lung epithelial adenocarcinoma A549 cells, inhibiting tumor angiogenesis (Ye et al. 2008). Because H_2O_2 stimulates both tumor angiogenesis and invasion, ERW may also suppress MMP-2 activation in A549 cells. ERW induced drastic morphological changes concomitant with telomere shortening in A549 cells and human uterine cancer HeLa cells but not in human normal fibroblast TIG-1 cells after cultivation for 90 days, although ERW suppressed the growth of cancer cells more strongly than that of TIG-1 cells (Shirahata et al. 1999). So far the safety of ERW has been repeatedly demonstrated in animals and humans (Shirahata et al. 2012). Whether ERW affects the production of MMP-2 in normal and cancer cells in different manners is an interesting issue and remains to be investigated in the future. ERW can be easily consumed in daily life and may be a promising antioxidant for the prevention and improved treatment of cancers.

References

Adler A, Yin Z, Tew KD, Ronai Z (1999) Role of redox potential and reactive oxygen species in stress signaling. Oncogene 18:6104–6111

Aiken JD III, Finke RG (1999) A review of modern transition-metal nanoclusters: their synthesis, characterization, and application in catalysis. J Mol Catal A-Chem 145:1–44

Albini A, D'Agostini F, Giunciuglio D, Paglieri I, Balansky R, De Flora S (1995) Inhibition of invasion, gelatinase activity, tumor take and metastasis of malignant cells by N-acetylcysteine. Int J Cancer 61:121–129

Aruoma OI, Halliwell B, Hoey BM, Butler J (1989) The anti-oxidant action of n-acetylcysteine: with hydrogen perox-ide, hydroxyl radical, and hypochlorous acid its reaction superoxide. Free Radic Biol Med 6:593–597

Belkhiri A, Richards C, Whaley M, McQueen SA, Orr W (1997) Increased expression of activated matrix metalloprotein-ase-2 by human endothelial cells after sublethal H_2O_2 exposure. Lab Invest 77:533–539

Bian J, Sun Y (1997) Transcriptional activation by p53 of the human type IV collagenase (gelatinase A or matrix metalloproteinase 2) promoter. Mol Cell Biol 17:6330–6338

Cai T, Fassina GF, Morini M, Grazia M, Aluigi G, Masiello L, Fontanini G, D'Agostini F, De Flora S, Noonan DM, Albini A (1999) N-acetylsysteine inhibits endothelial cell inva-sion and angiogenesis. Lab Invest 79:1151–1159

Chaiswing L, Zhong W, Liang Y, Jones DP, Oberley TD (2012) Regulation of prostate cancer cell invasion by modulation of extra- and intracellular redox balance. Free Radic Biol Med 52:452–461

Chithrani DB (2010) Intracellular uptake, transport, and pro-cessing of gold nanostructures. Mol Membr Biol 27:299–311

Dayem AA, Choi H-Y, Kim J-H, Cho S-G (2010) Role of oxi-dative stress in stem, cancer, and cancer stem cells. Cancers 2:854–884

Duarte TL, Almeida GM, Jones GDD (2007) Investigation of the role of extracellular H_2O_2 and transition metal ions in the genotoxic action of ascorbic acid in cell culture models. Toxicol Lett 170:57–65

Fisher KE, Pop A, Koh W, Anthis NJ, Saunders WB, Davis GE (2006) Tumor cell invasion of collagen matrices requires coordinate lipid agonist-induced G-protein and membrane-type matrix metalloproteinase-1-dependent signaling. Mol Cancer 5:69

Forget MA, Desrosiersand RR, Beliveau R (1999) Physiological roles of matrix metalloproteinases: implications for tumor growth and metastasis. Can J Physiol Pharmacol 77:465–480

Fujita K, Seike T, Yutsudo N, Ohno M, Yamada H, Yamaguci H, Sakumi K, Yamakawa Y, Kido M, Takaki A, Katafuchi T, Tanaka Y, Nakabeppu Y, Noda M (2009) Hydrogen in drinking water reduces dopaminergic neuronal loss in the 1-methyl-4-phenyl-1,2,3,6- tetrahydropyridine mouse model of Parkinson's disease. PLoS ONE 4:e7247

Gehrke H, Pelka J, Hartinger CG, Blank H, Bleimund F, Schneider R, Gerthsen D, Bräse S, Crone M, Türk M, Marko D (2011) Platinum nanoparticles and their cellular uptake and DNA platination at non-cytotoxic concentra-tions. Arch Toxicol 85:799–812

Hadi SM, Ullah MF, Shamim U, Bhartt SH, Azmi AS (2010) Catalytic therapy of cancer by ascorbic acid involves redox cycling of exogenous/endogenous copper ions and gener-ation of reactive oxygen species. Chemotherapy 56:280–284

Hamasaki H, Kashiwagi T, Imada I, Nakamichi N, Aramaki S, Toh S, Morisawa S, Shimakoshi H, Hisaeda Y, Shirahata S (2008) Kinetic analysis of superoxide anion radical-scav-enging and hydroxyl radical-scavenging activities of plat-inum nanoparticles. Langmuir 24:7354–7364

Hirakawa N, Miura Y, Yagasaki K (2005) Inhibitory effect of ascorbic acid on the proliferation and invasion of hepatoma cells in culture. Cytotechnology 47:133–138

Huang KC, Yang CC, Lee KT, Chien CT (2003) Reduced he-modialysis-induced oxidative stress in end-stage renal disease patients by electrolyzed reduced water. Kidney Int 64:704–714

Hwang YP, Yun HJ, Choi JH, Han EH, Kim HG, Song GY, Kwon K-I, Jeong TC, Jeong HG (2011) Suppression of EGF-induced tumor cell migration and matrix metallo-proteinase-9 expression by capsaicin via the inhibition of EGFR-mediated FAK/Akt, PKC/Raf/ERK, p38 MAPK, and AP-1 signaling. Mol Nutr Food Res 55:594–605

Isobe Y, Yamauchi M, Ikeda R, Kitagawa H (2003) A study on hydrogen adsorption of polymer protected Pt nanoparti-cles. Synth Met 135–136:757–758

Kajita M, Hikosaka K, Iitsuka M, Kanayama A, Toshima N, Miyamoto Y (2007) Platinum nanoparticle is a useful scavenger of superoxide anion and hydrogen peroxide. Free Radic Res 41:615–626

Kessenbrock K, Plaks V, Werb Z (2010) Matrix metallopro-teinases: regulators of the tumor microenvironment. Cell 141:52–67

Kim J, Takahashi M, Shimizu T, Shirasawa T, Kajita M, Kanayama A, Miyamoto Y (2008) Effects of a potent antioxidant, platinum nanoparticle, on the lifespan of *Caenorhabditis elegans*. Mech Ageing Dev 129:322–331

Kim K-H, Cho YS, Parka J-M, Yoon S-O, Kim K-W, Chung A-S (2007) Pro-MMP-2 activation by the PPARγ agonist, ciglitazone, induces cell invasion through the generation of ROS and the activation of ERK. FEBS Lett 581:3303–3310

Komatsu T, Katakura Y, Teruya K, Otsubo K, Morisawa S, Shirahata S (2004) Electrolyzed reduced water induces differentiation in K-562 human leukemia cells. In: Yaga-saki K et al (eds) Animal cell technology: basic & applied aspects. Kluwer, The Netherlands, pp 387–391

Krpetić Ž, Porta F, Caneva E, Dal Santo V, Scarì G (2010) Phagocytosis of biocompatible gold nanoparticles. Lang-muir 26:14799–14805

Kyaw M, Yoshizumi M, Tsuchiya K, Izawa Y, Kanematsu Y, Fujita Y, Ali N, Ishizawa K, Yamauchi A, Tamaki T (2004) Antioxidant effects of stereoisomers of *N*-Acetylcysteine (NAC), L-NAC and D-NAC, on angiotensin II-stimulated MAP kinase activation and vascular smooth muscle cell proliferation. J Pharmacol Sci 95:483–486

Ladiges W, Wanagat J, Preston B, Loeb L, Rabinovitch P (2010) A mitochondrial view of aging, reactive oxygen species and metastatic cancer. Aging Cell 9:462–465

Li Y, Nishimura T, Teruya K, Maki T, Komatsu T, Hamasaki T, Kashiwagi T, Kabayama S, Shim SY, Katakura Y, Osada K, Kawahara T, Otsubo K, Morisawa S, Ishii Y, Gadek Z, Shirahata S (2002) Protective mechanism of reduced water against alloxan-induced pancreatic β-cell damage: scavenging effect against reactive oxygen species. Cytotechnology 40:139–149

Li Y, Hamasaki T, Nakamichi N, Kashiwagi T, Komatsu T, Ye J, Teruya K, Abe M, Yan H, Kinjo T, Kabayama S, Kawamura M, Shirahata S (2011) Suppressive effects of electrolyzed reduced water on alloxan-induced apoptosis and type 1 diabetes mellitus. Cytotechnology 63:119–131

Liou G-Y, Storz P (2010) Reactive oxygen species in cancer. Free Radic Res 44:479–496

Ma X, Wu Y, Jin S, Tian Y, Zhang X, Zhao Y, Yu L, Liang X-J (2011) Gold nanoparticles induce autophagosome accumulation through size-dependent nanoparticle uptake and lysosome impairment. ACS Nano 5:8629–8639

Maeda H, Fukuyasu Y, Yoshida S, Fukuda M, Saeki K, Matsuno H, Yamauchi Y, Yoshida K, Hirata K, Miyamoto K (2004) Fluorescent probes for hydrogen peroxide based on a non-oxidative mechanism. Angew Chem Int Ed 43:2389–2391

Maxova H, Bacakova L, Lisa V, Novotna J, Tomasova H, Vizek M, Herget J (2010) Production of proteolytic enzymes in mast cells, fibroblasts, vascular smooth muscle and endothelial cells cultivated under normoxic or hypoxic conditions. Phys Res 59:711–719

Minaev B, Ågren H (1999) Spin uncoupling in molecular hydrogen activation by platinum clusters. J Mol Catal A 149:179–195

Mook ORF, Frederiks WM, Van Noorden CJ (2004) The role of gelatinases in colorectal cancer progression and metastasis. Biochim Biophys Acta 1705:69–89

Nelson KK, Melendez JA (2004) Mitochondrial redox control of matrix metalloproteinases. Free Radic Biol Med 37:768–784

Nguyen HL, Zucker S, Zarrabi K, Kadam P, Schmidt C, Cao J (2011) Oxidative stress and prostate cancer progression are elicited by membrane-type 1 matrix metalloproteinase. Mol Cancer Res 9:1305–1318

Nishikawa R, Teruya K, Katakura Y, Osada K, Hamasaki T, Kashiwagi T, Komatsu T, Li Y, Ye J, Ichikawa A, Otsubo K, Morisawa S, Xu Q, Shirahata S (2005) Electrolyzed reduced water supplemented with platinum nanoparticles suppresses promotion of two-stage cell transformation. Cytotechnology 47:97–105

Oda M, Kusumoto K, Teruya K, Hara T, Maki T, Kabayama Y, Katakura Y, Otsubo K, Morisawa S, Hayashi H, Ishii Y, Shirahata S (1999) Electrolyzed and natural reduced water exhibit insulin-like activity on glucose uptake into muscle cells and adipocytes. In: Bernard A et al (eds) Animal cell technology: products from cells, cells as products. Kluwer, The Netherlands, pp 425–427

Ortega AL, Mena S, Estrela JM (2010) Oxidative and nitrosative stress in the metastatic microenvironment. Cancers 2:274–304

Park MJ, Park IC, Hur JH, Kim MS, Lee HC, Woo SH, Lee KH, Rhee CH, Hong SI, Lee SH (2002) Modulation of phorbol ester-induced regulation of matrix metalloproteinases and tissue inhibitors of metalloproteinases by SB203580, a specific inhibitor of p38 mitogen-activated protein kinase. J Neurosurg 97:112–118

Pelka J, Gehrke H, Esselen M, Türk M, Crone M, Bräse S, Muller T, Blank H, Send W, Zibat V, Brenner P, Schneider R, Gerthsen D, Marko D (2009) Cellular uptake of platinum nanoparticles in human colon carcinoma cells and their impact on cellular redox systems and DNA integrity. Chem Res Toxicol 22:649–659

Qin H, Sun Y, Benveniste EN (1999) The transcription factors Sp1, Sp3, and AP-2 are required for constitutive matrix metalloproteinase-2 gene expression in astroglioma cells. J Biol Chem 274:29130–29137

Roh MR, Zheng Z, Kim HS, Kwon JE, Jeung HC, Rha SY, Chung KY (2012) Differential expression patterns of MMPs and their role in the invasion of epithelial premalignant tumors and invasive cutaneous squamous cell carcinoma. Exp Mol Pathol 92:236–242

Roomi MW, Kalinovsky T, Rath M, Niedzwiecki A (2011) Down-regulation of urokinase plasminogen activator and matrix metalloproteinases and up-regulation of their inhibitors by a novel nutrient mixture in human prostate cancer cell lines PC-3 and DU-145. Oncol Rep 26:1407–1413

Roucoux A, Schulz J, Patin H (2002) Reduced transition metal colloids: a novel family of reusable catalysts? Chem Rev 102:3757–3778

Schumacker PT (2006) Reactive oxygen species in cancer cells: live by the sword, die by the sword. Cancer Cell 10:175–176

Shan Y, Ma S, Nie L, Shang X, Hao X, Tang Z, Wang H (2011) Size-dependent endocytosis of single gold nanoparticles. Chem Commun 47:8091–8093

Shcherbachenko IM, Lisovskaya IL, Tikhonov VP (2007) Oxidation-induced calcium-dependent dehydration of normal human red blood cells. Free Radic Res 41:536–545

Shirahata S (2002) Reduced water for prevention of disease. In: Shirahata S, Teruya K, Katakura Y (eds) "Animal Cell Technology: Basic & Applied Aspects". Proceedings of the 13th JAACT meeting, 16–21 November, 2000. Kluwer, Fukuoka-Karatsu, pp 25–30

Shirahata S, Kabayama S, Nakano M, Miura T, Kusumoto K, Gotoh M, Hayashi H, Otsubo K, Morisawa S, Katakura Y (1997) Electrolyzed-reduced water scavenges active oxygen species and protects DNA from oxidative damage. Biochem Biophys Res Commun 234:269–274

Shirahata S, Murakami E, Kusumoto K, Yamashita M, Oda M, Teruya K, Kabayama S, Otsubo K, Morisawa S, Hayashi H, Katakura Y (1999) Telomere shortening in cancer cells by electrolyzed-reduced water. In: Ikura K, Nagao M, Masuda S, Sasaki R (eds) Animal cell technology: challenges for the 21st century. Kluwer, The Netherlands, pp 355–359

Shirahata S, Hamasaki T, Haramaki K, Nakamura T, Abe M, Yan H, Kinjo T, Nakamichi N, Kabayama S, Teruya K (2011) Anti-diabetes effect of water containing hydrogen molecule and Pt nanoparticles. BMC Proc 5:18–20

Shirahata S, Hamasaki T, Teruya K (2012) Advanced research on the health benefit of reduced water. Trends Food Sci Technol 23:123–131

Shukla R, Bansal V, Chaudhary M, Basu A, Bhonde RR, Sastry M (2005) Biocompatibility of gold nanoparticles and their endocytotic fate inside the cellular compartment: a microscopic overview. Langmuir 21:10644–10654

Sternlicht MD, Werb Z (2001) How matrix metalloproteinases regulate cell behavior. Annu Rev Cell Dev Biol 17: 463–516

Strongin AY, Marmer BL, Grant GA, Goldberg GI (1993) Plasma membrane-dependent activation of the 72-kDa type IV collagenase is prevented by complex formation with TIMP-2. J Biol Chem 268:14033–14039

Szatrowski TP, Nathan CF (1991) Production of large amounts of hydrogen peroxide by human tumor cells. Cancer Res 51:794–798

Taylor U, Klein S, Petersen S, Kues W, Barcikowski S, Rath D (2010) Nonendosomal cellular uptake of ligand-free, positively charged gold nanoparticles. Cytometry 77A:439–446

Tsai CF, Hsu YW, Chen WK, Ho YC, Lu FJ (2009a) Enhanced induction of mitochondrial damage and apoptosis in human leukemia HL-60 cells due to electrolyzed-reduced water and glutathione. Biosci Biotechnol Biochem 73:280–287

Tsai CF, Hsu YW, Chen WK, Chang WH, Yen CC, Ho YC, Lu FJ (2009b) Hepatoprotective effect of electrolyzed reduced water against carbon tetrachloride-induced liver damage in mice. Food Chem Toxicol 47:2031–2036

Vayalil PK, Elmets CA, Katiyar SK (2003) Treatment of green tea polyphenols in hydrophilic cream prevents UVB-induced oxidation of lipids and proteins, depletion of antioxidant enzymes and phosphorylation of MAPK proteins in SKH-1 hairless mouse skin. Carcinogenesis 24:927–936

Wang J, Yi J (2008) Cancer cell killing via ROS. Cancer Biol Ther 7:1875–1884

Watzky MA, Finke RG (1997) Transition metal nanocluster formation kinetic and mechanistic studies. A new mechanism when hydrogen is the reductant: slow, continuous nucleation and fast autocatalytic surface growth. J Am Chem Soc 119:10382–10400

Wondrak GT (2009) Redox-directed cancer therapeutics: molecular mechanisms and opportunities. Antioxid Redox Signal 11:3013–3069

Wu W-S (2006) The signaling mechanism of ROS in tumor progression. Cancer Metast Rev 25:695–705

Yan H, Tian H, Kinjo T, Hamasaki T, Tomimatsu K, Nakamichi N, Teruya K, Kabayama S, Shirahata S (2010) Extension of the lifespan of Caenorhabditis elegans by the use of electrolyzed reduced water. Biosci Biotechnol Biochem 74:2011–2015

Yan H, Kinjo T, Tian H, Hamasaki T, Teruya K, Kabayama S, Shirahata S (2011) Mechanism of the lifespan extension of Caenorhabditis elegans by electrolyzed reduced water–participation of Pt nanoparticles. Biosci Biotechnol Biochem 75:1295–1299

Ye J, Li Y, Hamasaki T, Nakamichi N, Komatsu T, Kashiwagi T, Teruya K, Nishikawa R, Kawahara T, Osada K, Toh K, Abe M, Tian H, Kabayama S, Otsubo K, Morisawa S, Katakura Y, Shirahata S (2008) Inhibitory effect of electrolyzed reduced water on tumor angiogenesis. Biol Pharm Bull 31:19–26

Yeom C-H, Lee G, Park J-H, Yu J, Park S, Yi S-Y, Lee HR, Hong YS, Yang J, Lee S (2009) High dose concentration administration of ascorbic acid inhibits tumor growth in BALB/C mice implanted with sarcoma 180 cancer cells via the restriction of angiogenesis. J Transl Med 7:70

Yoon SO, Park SJ, Yoon SY, Yun CH, Chung AS (2002) Sustained production of H_2O_2 activates pro-matrix metalloproteinase-2 through receptor tyrosine kinases/phosphatidylinositol 3-kinase/NF-kappa B pathway. J Biol Chem 277:30271–30282

Yoshihisa Y, Zhao Q-L, Hassan MA, Wei Z-L, Furuichi M, Miyamoto Y, Kondo T, Shimizu T (2011) SOD/catalase mimetic platinum nanoparticles inhibit heat-induced apoptosis in human lymphoma U937 and HH cells. Free Radic Biol Med 45:326–335

Zafarullah M, Li WQ, Sylvester J, Ahmad M (2003) Molecular mechanisms of N-acetylcysteine actions. Cell Mol Life Sci 60:6–20

Zhang HJ, Zhao W, Venkataraman S, Robbins MEC, Buettner GR, Kregel KC, Oberley LW (2002) Activation of matrix metalloproteinase-2 by overexpression of manganese superoxide dismutase in human breast cancer MCF-7 cells involves reactive oxygen species. J Biol Chem 277:20919–20926

Zhang L, Fischer W, Pippel E, Hause G, Brandsch M, Knez M (2011) Receptor-mediated cellular uptake of nanoparticles: a switchable delivery system. Small 7:1538–1541